AIP | Applied Physics Letters

Defect-free 100-layer strain-balanced InAs quantum dot structure grown on InP substrate

Z. H. Zhang, K. Y. Cheng, C. F. Xu, and K. C. Hsieh

Citation: Appl. Phys. Lett. **89**, 063115 (2006); doi: 10.1063/1.2335605
View online: http://dx.doi.org/10.1063/1.2335605
View Table of Contents: http://apl.aip.org/resource/1/APPLAB/v89/i6
Published by the American Institute of Physics.

Defect-free 100-layer strain-balanced InAs quantum dot structure grown on InP substrate

Z. H. Zhang, K. Y. Cheng,[a] C. F. Xu, and K. C. Hsieh
Department of Electrical and Computer Engineering, University of Illinois at Urbana-Champaign, Urbana, Illinois 61801 and Micro and Nanotechnology Laboratory, University of Illinois at Urbana-Champaign, Urbana, Illinois 61801

(Received 29 December 2005; accepted 2 July 2006; published online 9 August 2006)

A high quality 100-layer InAs quantum dot (QD) structure was successfully grown on InP substrate. The overall compressive strain caused by InAs QDs on InAlGaAs/InP is effectively balanced by inserting tensile-strained InGaAs strain-balance layers immediately above QD layers. The cross-sectional transmission electron microscopy images show a low defect density of less than 10^6 cm^{-2} and a smooth interface between QD layers throughout the whole structure. In addition, the intense room temperature photoluminescence indicates a good optical quality of the multilayer QD structure. © *2006 American Institute of Physics*. [DOI: 10.1063/1.2335605]

Quantum well infrared photodetectors (QWIPs) based on intersubband transitions in the conduction band or valence band of QWs have been rapidly developed for practical applications.[1] However, due to the quantum mechanical selection rules, QWIP is insensitive to normal incident lights. Furthermore, QWIP is limited by the short photoexcited carrier lifetime for high temperature operation.[1] On the other hand, theoretical studies indicate that photodetectors based on quantum dot (QD) nanostructures have no polarization preference in light absorption and much longer carrier lifetime.[2] Unfortunately, current device performance lags behind the theoretical predictions, partially due to the difficulties encountered in the growth control of the self-assembled QDs. Because of the stochastic nature of the self-assembled QD formation through Stranski-Krastanow growth mode, an accurate control of the size, shape, and density of QDs cannot be obtained. As a consequence, the exact electronic structure of the QDs is difficult to predict for the optimization of the photodetector, resulting in a low responsivity of the current QD infrared photodetectors (QDIPs). One of the tractable methods to improve the device performance is to employ structures with multiple, vertically stacked QD layers, which improve the uniformity of the QD size distribution.[3] The multilayer structure also effectively increase the absorption volume of the incident photons.[4,5] However, the accumulation of strain in QD arrays prohibits the stacking of a large number of QD layers without the generation of defects. A thick barrier (⩾500 Å) layer is usually used to release the strain and, thus, to reduce the generation of defects in the structure. But the reduced strain field in thick barrier layer is less effective in improving the uniformity of the QDs. In order to solve the strain accumulation problem, we demonstrated that, even in structures with thin (150 Å) barrier layers, the overall compressive strain in a multilayer QD structure can be controlled by incorporating properly designed tensile strain layers adjacent to QD layers.[6] In this study, the strain-balanced QD system was used to fabricate a defect-free 100-layer strain-balanced InAs QD structure self-assembled on InAlGaAs/InP. The high optical and structural qualities of this sample show a great potential of using the strain-balanced QD system in fabricating high performance photonic devices.

Samples used in this work were grown in a solid-source molecular beam epitaxy system on sulfur-doped (100) InP substrates. The growth temperature was measured with a pyrometer, which was calibrated with the InP surface oxide desorption temperature of 500 °C. The structure consists of a 20-period $In_{0.52}Al_{0.48}As/In_{0.53}Ga_{0.47}As$ buffer superlattice and a 1 μm $In_{0.52}Al_{0.34}Ga_{0.14}As$ buffer layer grown at 510 °C with the arsenic overpressure of 2×10^{-6} Torr. The growth rate for InAlGaAs layer was set to 1 μm/h. The buffer superlattice and the buffer layer were doped with silicon to a carrier concentration of 1×10^{18} cm^{-3}. Following the buffer layer growth, a 1000 Å undoped InAlGaAs bottom confinement layer was grown. The growth temperature was gradually decreased to 480 °C and the arsenic overpressure was dropped to 1.5×10^{-6} Torr during the growth of the bottom InAlGaAs confinement layer for preparation of QD growth. The active region of the sample was formed by periodically repeating the 5 ML of InAs QD layer, the 5.5 ML tensile strained $In_{0.2}Ga_{0.8}As$ strain balance layer (SBL), and the 500 Å InAlGaAs barrier layer. Before the deposition of each InAs layer, a 30 s growth interruption under an arsenic flux was inserted to stabilize the surface of the matrix layer. The InAs layer was then deposited at 480 °C with an arsenic overpressure of 1.5×10^{-6} Torr to form self-assembled QDs. A low growth rate of 0.06 ML/s for InAs QD deposition was used to increase the density and uniformity of the QDs.[7] Each QD layer was δ doped using silicon to an equivalent three-dimensional (3D) electron concentration of 3×10^{17} cm^{-3}. After the deposition of each InAs layer, another 30 s interruption under an arsenic flux was used and followed by the growth of the InGaAs SBL and InAlGaAs barrier layer at the same temperature and arsenic overpressure. After the growth of the 100-period QD active region, an undoped 1000 Å InAlGaAs top confinement layer and a 4000 Å InAlGaAs layer doped with silicon to a carrier concentration of 1×10^{18} cm^{-3} were grown. Finally, a 1500 Å InGaAs contact layer doped with silicon to a carrier concentration of 5×10^{18} cm^{-3} was deposited to cap the whole structure. Throughout the growth process, the substrate ma-

[a]Author to whom correspondence should be addressed; electronic mail: kycheng@uiuc.edu

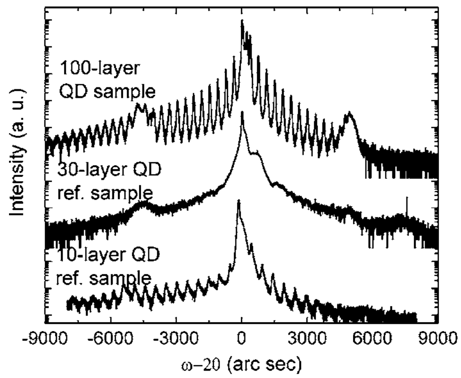

FIG. 1. HRXRD rocking curves of the 100-layer QD sample with InGaAs SBLs and the reference samples containing 10- and 30-layer QDs without InGaAs SBL. The peak with the highest intensity at 0° is from the InP substrate.

nipulator was rotated at about 4.4 rpm to achieve uniform film deposition.

The overall strain effects of the sample were studied by the high-resolution x-ray diffraction (HRXRD) measurements. Cross-sectional transmission electron microscopy (XTEM) was used to examine the microstructure and measure the defect density in the QD sample. The optical quality of the sample was characterized by both 300 and 77 K photoluminescence (PL) measurements. The excitation source of the PL measurements was the 514.5 nm line of an Ar^+ laser. A liquid nitrogen cooled Ge detector mounted on a 0.5 m spectrometer was used for detection in lock-in mode.

The overall strain in the 100-layer QD sample was studied first using HRXRD. Figure 1 shows the diffraction rocking curves for (004) reflection of the 100-layer QD sample. The diffraction rocking curves of two reference QD samples are also included for comparison. Both reference samples have identical structures as the 100-layer QD sample except that the active regions of the reference samples have 10 and 30 QD layers, respectively, and no InGaAs SBL was used. The highest intensity peak at 0° is from the InP substrate. The strong asymmetric distribution of the satellite peaks in the rocking curve of the ten-layer QD reference sample indicates the existence of an overall strain in the structure. The satellite peaks are distributed mainly on the left-hand side of the InP substrate peak, indicating a net compressive strain existing in the reference ten-layer QD sample. When stacking 30 QD layers without InGaAs SBL, the satellite peaks disappear and become indistinguishable from the background noise. This indicates the formation of corrugated growth front caused by the strain accumulation in the 30-layer QD reference sample as evident in the XTEM studies. However, the satellite peaks in the rocking curve of the 100-layer QD sample have high intensity, narrow linewidth, and consistent periodicity. These features indicate that the 100-layer QD sample maintains its structural integrity throughout the whole structure with very smooth interfaces and well-defined periodicity. In addition, the rocking curve of the 100-layer QD sample is more symmetric compared with the reference samples, indicating the overall compressive strain caused by InAs QDs is effectively balanced by the tensile-strained InGaAs SBLs. It should be pointed out that the two symmetric humps around ±4500 arc sec are due to the composition modulation in InAlGaAs layers caused by the asymmetric effusion cell locations coupled with the substrate rotation.

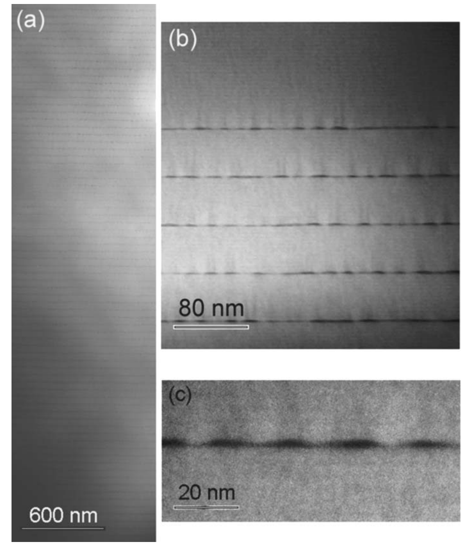

FIG. 2. Cross-sectional TEM micrographs of the 100-layer QD sample. (a) The center 75 QD layers. (b) The top five QD layers. (c) Zoom-in images of QD layers.

Due to the large active region thickness (>5 μm) of the 100-layer QD sample, it is difficult to show the complete structure in a single XTEM micrograph. A lower magnification TEM picture of the center 75 QD layers of the active region is shown in Fig. 2(a). Figure 2(b) shows the zoom-in image of the top five QD layers, indicating a defect-free multilayer QD structure with smooth interfaces between neighboring QD layers even at top QD layers. Figures 2(c) shows the detail image of the strain-balanced QD layers. The QD nanostructures have an average base diameter of around 200 Å and height of 20 Å, which are consistent with the atomic force microscopy results of QD samples without cap layer grown under a similar condition.[8] Furthermore, Figs. 2(b) and 2(c) also display a uniform QD size distribution in each QD layer and defect-free flat interfaces between QD layers. These data show the potential of the 100-layer QD sample in fabricating the high performance QDIP device.

Comparing the XTEM micrographs of the 30-layer QD reference sample (not shown) and the 100-layer QD sample (Fig. 2), two major structural improvements in the multilayer QD structure incorporating InGaAs SBLs are evident. First, the incorporation of SBL can efficiently suppress defects formation in strained multilayer QD structures. Due to the ac-

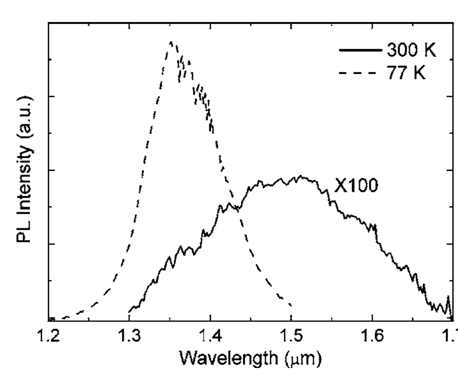

FIG. 3. Room temperature and 77 K photoluminescence spectra of the 100-layer QD sample grown on InAlGaAs/InP.

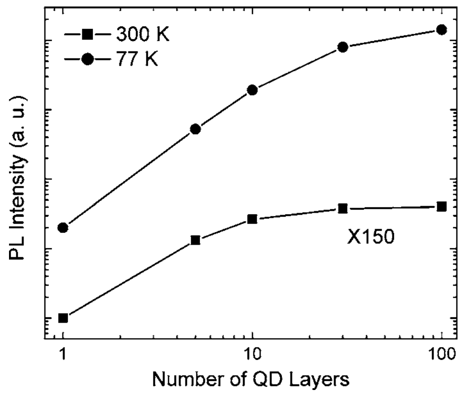

FIG. 4. Comparison of room temperature and 77 K photoluminescence intensities among QD samples containing various number of QD layers.

cumulation of compressive strain in the conventional multilayer QD structure, a large defect density of $\geqslant 10^9$ cm^{-2} in the 30-layer QD reference sample is observed. On the contrary, no visible defects are detected in the XTEM images of the 100-layer QD sample, as shown in Fig. 2, and the defect density is estimated to be less than 10^6 cm^{-2}. This indicates that the incorporation of the InGaAs SBLs can effectively balance the overall compressive strain and solved the defect generation problem caused by the strain accumulation.

The second structural improvement by incorporating the InGaAs SBLs in the 100-layer QD sample is the rapid formation of a smooth growth front after the QD deposition. Since the QD growth involves the transition from the two-dimensional layer-by-layer growth to 3D island growth, the multilayer QD structure requires the barrier layer on top of each QD layer to be smoothed out effectively in order to achieve high structural quality. However, when stacking a large number of QD layers, due to the strain buildup, the growth front becomes severely corrugated in the later stage of the QD structure. This leads to a nonplanar interface between neighboring layers. On the contrary, the smooth and straight interfaces between neighboring layers shown in Fig. 2 indicate that the growth front has been effectively smoothed out by the InGaAs SBL. This is supported by the observed reflection high energy electron diffraction (RHEED) patterns during the growth.[6] After the deposition of the InGaAs SBL, the spotty RHEED pattern formed after the QD formation became streaky again, indicating a smooth growth front ready for high quality InAlGaAs barrier layer deposition.

Figure 3 shows the PL spectra of the 100-layer QD sample with a peak wavelength centered at 1.51 and 1.35 μm at room temperature and 77 K, respectively. The PL spectra were measured after etching off the InGaAs contact layer. In order to evaluate the optical quality of the 100-layer QD sample, several QD samples with identical structure but containing less (1, 5, 10, and 30) QD layers in the active region were grown. As shown in Fig. 4, the increasing number of QD layers in the active region leads to higher PL intensities at both room temperature and 77 K. This indicates that the structural quality of QD samples does not degrade with more QD layers stacked in the active region. Besides, the strong room temperature PL intensity of the 100-layer QD sample proves that a low defect density in the structure has been achieved.

In conclusion, the defect-free 100-layer strain-balanced InAs QD structure was achieved on the InP substrate. HRXRD measurements revealed that the compressive strain caused by the QDs deposition has been effectively balanced by the tensile strained InGaAs SBLs. The XTEM measurements indicated a low defect density of less than 10^6 cm^{-2}. The smooth interface observed in the XTEM micrograph proves that the SBL can smooth out the growth front effectively and ensure a high crystal quality of the following InAlGaAs barrier layer. PL measurement results of the strain-balanced QD structure show strong optical intensities and a great potential in fabrication of high performance photodetectors.

This work was partially supported by the U.S. Army Research Office MURI program (DAAD19-01-1-0591) and DARPA University Photonics Research Centers program (Hyper-Uniform Nanophotonic Technologies Center, HR0011-04-1-0034). The TEM measurement in this work was carried out in the Center for Microanalysis of Materials, University of Illinois, which is partially supported by the U.S. Department of Energy under Grant No.DEFG02-91-ER45439.

[1] B. F. Levine, J. Appl. Phys. **74**, R1 (1993).
[2] V. Ryzhii, Semicond. Sci. Technol. **11**, 759 (1996).
[3] H. Heidemeyer, S. Kiravittaya, C. Müller, and N. Y. Jin-Phillipp, Appl. Phys. Lett. **80**, 1544 (2002).
[4] B. Kochmann, A. D. Stiff-Roberts, S. Chakrabarti, J. D. Phillips, S. Krishna, J. Singh, and P. Bhattacharya, IEEE J. Quantum Electron. **39**, 459 (2003).
[5] S. Chakrabarti, A. D. Stiff-Roberts, P. Bhattacharya, S. Gunapala, S. Bandara, S. B. Rafol, and S. W. Kennerly, IEEE Photonics Technol. Lett. **16**, 1361 (2004).
[6] Z. H. Zhang, C. F. Xu, K. C. Hsieh, and K. Y. Cheng, J. Cryst. Growth **278**, 61 (2005).
[7] T. Kaizu and K. Yamaguchi, Jpn. J. Appl. Phys., Part 1 **42**, 1705 (2003).
[8] Z. H. Zhang and K. Y. Cheng, J. Vac. Sci. Technol. B **22**, 1508 (2004).